



**HAL**  
open science

## From early microstructural evolution to intergranular crack propagation in SAC solders under thermomechanical fatigue

E. Ben Romdhane, P. Roumanille, A. Guédon-Gracia, S. Pin, P. Nguyen, H. Frémont

► **To cite this version:**

E. Ben Romdhane, P. Roumanille, A. Guédon-Gracia, S. Pin, P. Nguyen, et al.. From early microstructural evolution to intergranular crack propagation in SAC solders under thermomechanical fatigue. *Microelectronics Reliability*, 2021, pp.114288. 10.1016/j.microrel.2021.114288 . hal-03375843

**HAL Id: hal-03375843**

**<https://hal.science/hal-03375843>**

Submitted on 5 Jan 2024

**HAL** is a multi-disciplinary open access archive for the deposit and dissemination of scientific research documents, whether they are published or not. The documents may come from teaching and research institutions in France or abroad, or from public or private research centers.

L'archive ouverte pluridisciplinaire **HAL**, est destinée au dépôt et à la diffusion de documents scientifiques de niveau recherche, publiés ou non, émanant des établissements d'enseignement et de recherche français ou étrangers, des laboratoires publics ou privés.



Distributed under a Creative Commons Attribution - NonCommercial 4.0 International License

# From early microstructural evolution to intergranular crack propagation in SAC solders under thermomechanical fatigue

E. Ben Romdhane<sup>a,b\*</sup>, P. Roumanille<sup>a</sup>, A. Guédon-Gracia<sup>b</sup>, S. Pin<sup>a</sup>, P. Nguyen<sup>c</sup>,  
H. Frémont<sup>b</sup>

<sup>a</sup> *Institut de Recherche Technologique Saint-Exupéry, Toulouse, France*

<sup>b</sup> *IMS Laboratory, University of Bordeaux, Talence, France*

<sup>c</sup> *Elemca, Toulouse, France*

## Abstract

Due to the complexity of the initial microstructure of lead-free solder joints combined to a failure mechanism that is not yet fully understood, lifetime predictions of SnAgCu solder joints remain a challenging task. In this work, Sn3.0Ag0.5Cu (SAC305) solder joints microstructural evolution during thermal cycling is presented. Electron Back Scattered Diffraction (EBSD) analyses were conducted to assess the SAC305 microstructure changes corresponding to different number of thermal cycles. The goal is to define the role of each microstructural phenomenon in the solder joint fatigue life by correlation with electrical failure monitoring results along the cycling test. Experimental observations show that crack initiation starts very early and precedes the propagation of  $\beta$ -Sn grains recrystallization in the solder high strain area. However, solder joint lifetime is controlled by recrystallization and  $\text{Ag}_3\text{Sn}$  particles coarsening which are the most important phenomena leading to the intergranular crack propagation.

## 1. Introduction

Reliability of solder joints under thermomechanical fatigue remains a major challenge with the ban on the use of lead by the RoHs directive in electronic applications and its replacement by lead-free SnAgCu alloys. Intergranular crack propagation is one of the frequent failure modes present in thermomechanical fatigue of SAC solder joint.

When a lead-free solder joint is exposed to thermal cycling, new smaller  $\beta$ -Sn grains appear through the recrystallization phenomenon due to viscoplastic strains. A recovery process takes place prior to recrystallization. Dislocations annihilate and rearrange to form low disorientated grains in high strain regions of solder joints [1]. These dislocation cells can then grow due to thermally activated and strain-enhanced  $\text{Ag}_3\text{Sn}$  coalescence, decreasing their surface energy, and rotate to generate a network of higher misorientated grains leading to a recrystallized region. This network represents a highly stressed area that promotes intergranular crack propagation until failure[2][3][4].

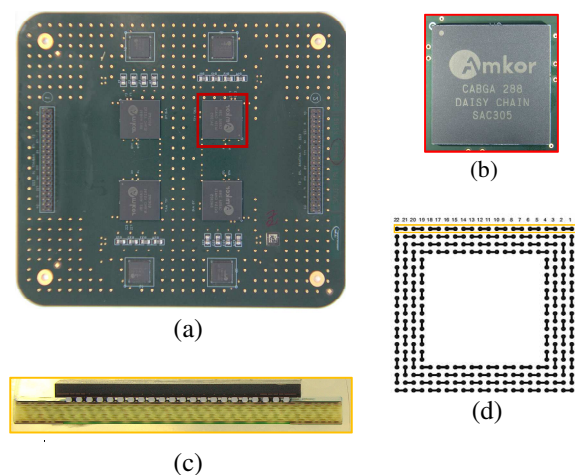


Figure 1 : Test vehicle with the BGA components studied in this work

While most studies focus on the microstructural process leading to the intergranular cracks propagation like recrystallization and  $\text{Ag}_3\text{Sn}$  intermetallic coalescence, few studies are interested in the phase of crack initiation and their impact on SAC solder joints service life.

\* emna.ben.romdhane@irt-saintexupery.com

In this paper, an in-depth microstructural investigation of the evolving SAC305 microstructure during the first aging cycles is presented. The main objective is to characterise each process leading to thermomechanical fatigue cracking and the link between the early stages of recrystallization and the time to crack initiation. The microstructural features evolution is studied to look for early damage indicators that can be exploited in life prediction models and to correlate with failure detection results.

## 2. Experimental procedure

The microstructural evolution during thermomechanical fatigue tests in solder joints of Chip Array Ball Grid Array (CABGA Amkor) components is evaluated. The package body size is 19 mm x 19 mm and the die size is 12mm x 12mm. There are 288 solder joints per BGA and each joint is 480  $\mu\text{m}$  in diameter with a 800  $\mu\text{m}$  pitch. Solder pads on the components have Electroless Nickel Immersion Gold (ENIG) finish with a solder mask defined (SMD) configuration. The components were soldered to a 1.6 mm FR-4 printed circuit board (PCB) with ENIG surface finish on non-solder mask defined (NSMD) pads. The board was also equipped with two connectors allowing the electrical monitoring of components during thermal cycling (Figure 1.a and Figure 1.b).

SAC305 solder paste was used in the surface mount assembly process with a time over liquidus of 75 s, a peak temperature of 245°C, and a cooling rate of 3°C/s.

The objective is to have a common test vehicle allowing the study of the microstructural evolution of solder joints as well as the number of cycles to failure for each of the components.

The thermal cycling was performed between -55°C and +125°C. The temperature ramp was 10°C/min and the dwell was 15 min.

Successive sampling was performed until 1700 cycles. The dates of sample withdraw were set based on the estimated average lifetime of the components under same accelerated test conditions. Samples are followed by metallographic investigations using white/polarized light microscopy and Scanning Electron Microscopy (SEM) observations along with EBSD analysis of solder joints after cross-sectioning in order to detect cracking as well as the degradation mechanism.

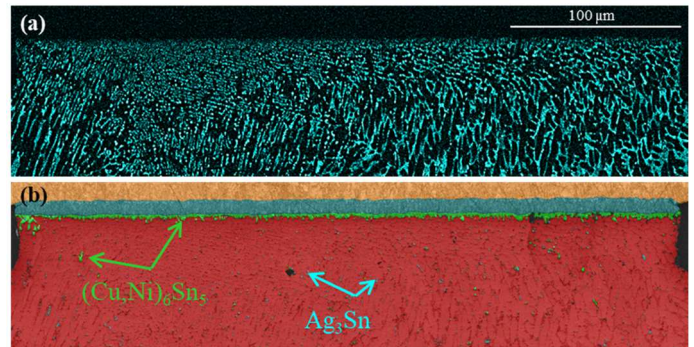


Figure 2 : As-reflowed BGA solder joint characterization, silver EDX (a) and crystalline phases maps

The degradation is defined as the change in the initial microstructure leading to the formation of the new tin grains as well as  $\text{Ag}_3\text{Sn}$  intermetallic coalescence. This evolution is characteristic of the solder fatigue: this paper will show that it can be used as an early failure indicator.

For optical microscopy, a Zeiss Axio Observer optical microscope equipped with a polarizer was used. The EBSD analysis was performed using a Zeiss Supra 55 VP SEM with a scan step of 0.4  $\mu\text{m}$ . EBSD data were then post-processed using the Aztec and Channel 5 softwares from Oxford Instruments.

At each sampling, 22 joints of the outermost row of two components were observed under optical microscope (Figure 1.c and Figure 1.d). The comparison of the different solder joints at the same level of cycling with white and polarized lights allowed us to choose the most representative cases to deepen the microstructural characterization by EBSD.

## 3. Results

### 3.1. $\beta$ -Sn grain structure in as-reflowed SAC305 CABGA solder joint

The as-reflowed microstructure of SAC305 solder joints and their mechanical properties depend on the conditions of reflow and the reactions taking place during the solidification of the SnAgCu solder alloy. It gives a  $\beta$ -Sn tin matrix with a dendritic structure and fine  $\text{Ag}_3\text{Sn}$  particles in the eutectic regions. The inter-dendritic spaces are characterized by the presence of  $(\text{Cu,Ni})_6\text{Sn}_5$  intermetallic compounds, which are larger than  $\text{Ag}_3\text{Sn}$  particles.

The presence of nickel in these precipitates depends on the amount of dissolved nickel from the finishes on the component and PCB pads. Nickel also participates to the formation of intermetallic layers at the component and PCB interfaces. The layers are also composed of  $(\text{Cu,Ni})_6\text{Sn}_5$  IMCs, depending on the quantity of nickel (Figure 2).

SAC solder joints microstructure after reflow presents also a random distribution with very varied morphologies. Observations show that the as-reflowed microstructure consists of few large  $\beta$ -Sn grains and can be described as:

- Macro-grained morphology that contains one or more  $\beta$ -Sn grains with different crystalline orientations. The size of these macrograins is of the same order of magnitude of the joint's one (Figure 3).
- Cyclic twinned morphology (also known as beach ball structure) which is referred to a highly textured microstructure consisting in three major twin orientations, which cyclically repeat about  $60^\circ$  around the  $[001]$  axis.
- Mixed morphology that is characterized by the presence of both the cyclic and interlaced twinned morphologies that are known to be due to the sixfold twinning of tin. The interlaced structures were often localized near the interface between the solder and the copper pad on component or PCB side and at the nucleation site of the beach ball structure (Figure 3).

The occurrence of these morphologies in BGA components depends on solder volume, alloy composition, surface finish and cooling rate [5].

As the initial microstructure is expected to have an impact on the thermomechanical response of lead-free solder joint due to tin grain anisotropy [6],[7], a quantitative study was made on different components. The single grain morphology measured on similar samples have been reported to be predominant with a percentage that may range up to 90 %, and not lower than 75% [8]. This percentage can be an overestimated because of the observation performed in a single plane. Nevertheless this justifies the study to focus on single grained joints.

### 3.2. Microstructure Evolution with Thermal Cycling

#### 3.2.1 Method of observation

In this study, the macrograin morphology was selected to follow the microstructural degradation phenomena and cracking in BGA solder joints. It is the simplest case allowing the study of the evolution of the different microstructural properties.

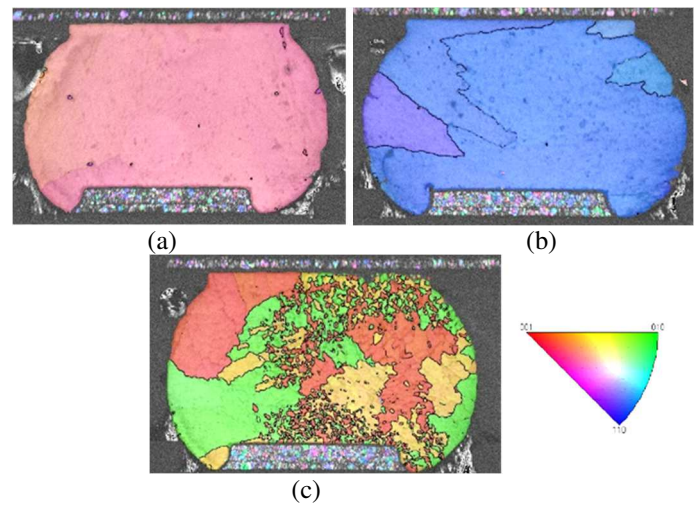


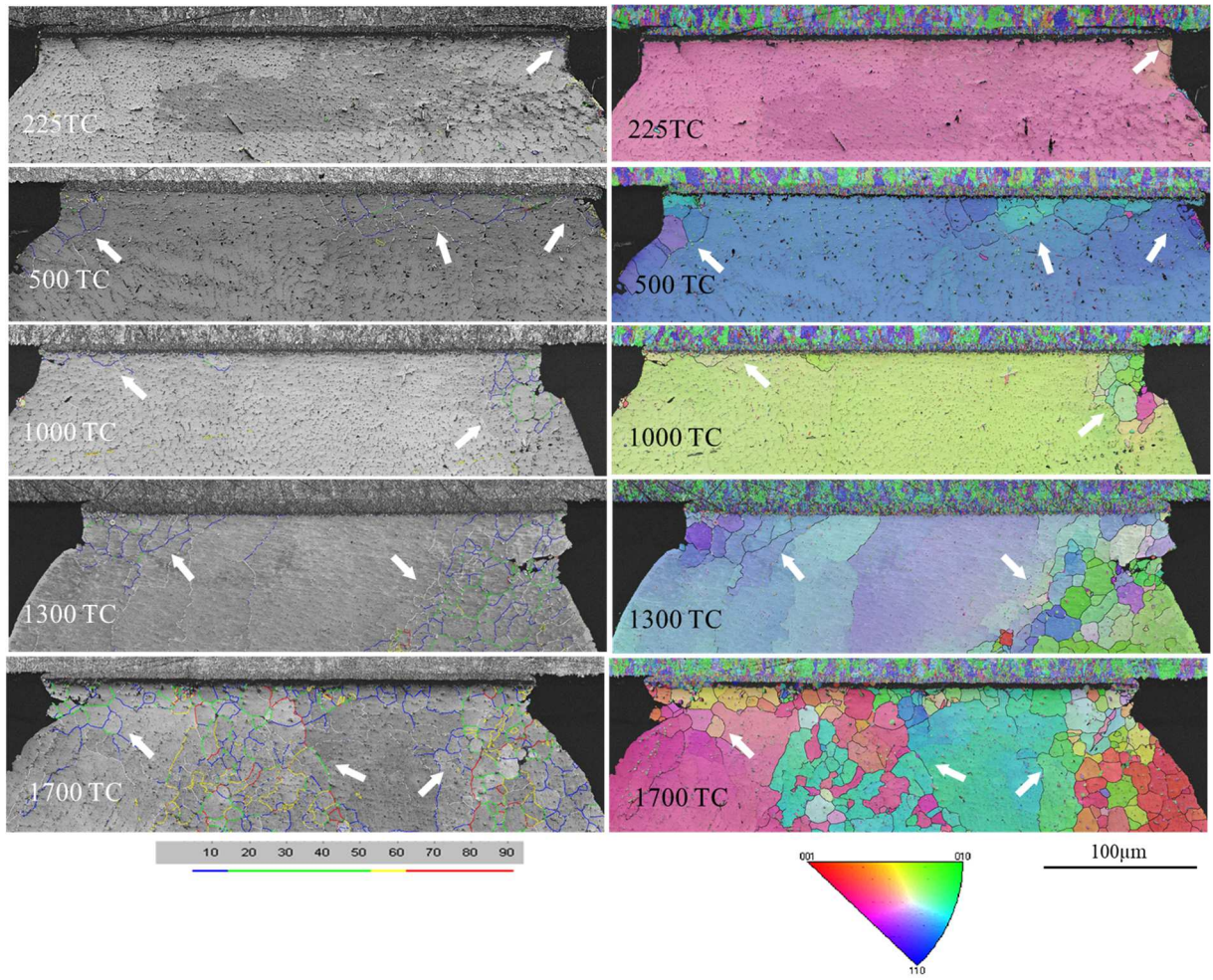
Figure 3. Different morphologies observed in as-reflowed solder joints, (a) single-grained, (b) poly-grained, (c) mixed

Multi-joints EBSD analyses on the corner joint and its four neighbors have been performed in a first time to check microstructural evolution at each sampling. The objective of this analysis is to calculate the recrystallization ratio in each joint and to compare the microstructural evolution in the various neighboring bumps. The most recrystallized sample was then selected for an EBSD analysis in the highest stressed region. Indeed, total cracks usually develop in these most recrystallized regions [9]. High magnification was chosen to permit a quantitative study of different microstructural features ( $\beta$ -Sn grain size and crystallographic orientation, grain boundary misorientation as well as  $\text{Ag}_3\text{Sn}$  IMC size).

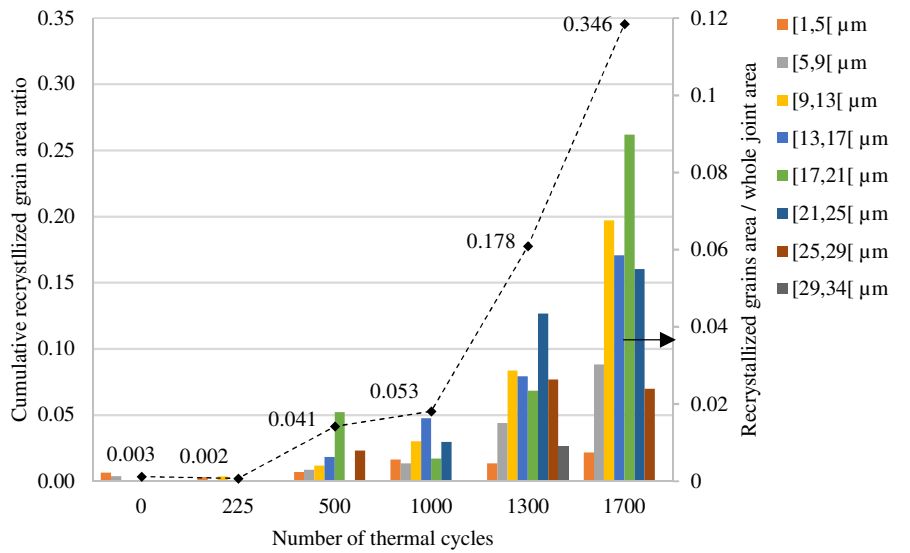
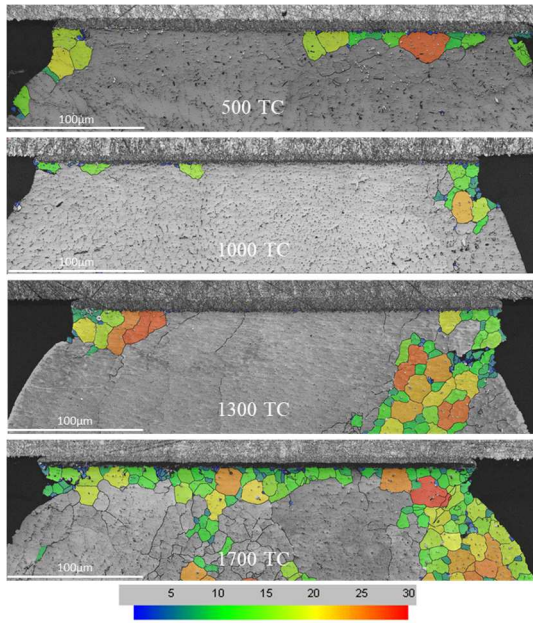
#### 3.2.2 Evolution of the $\beta$ -Sn grains

Microstructural analyses have been performed on components taken out of the thermal chamber during the first temperature cycles (0 – 1700 cycles) to set up the successive steps of recrystallization and its propagation in the solder joint. EBSD analysis showed that solder degradation has already started before 225 cycles. A recovery process has begun by the formation of  $\beta$ -Sn sub-grains (misorientation  $<5^\circ$ ) and low disorientated grains ( $<15^\circ$ ) in the most stressed area at the solder neck (Figure 4). These low grain boundaries angles were not detected in as-reflowed solder EBSD maps. Then tin recrystallization starts in the critical strain zone after 500 cycles. Grain boundaries with larger angles ( $>15^\circ$ ) appear and delimit new tin grains along the solder pads.





(a) (b)  
 Figure 4 : Evolution of the SAC305 solder joints after several thermal cycles, (a) grain boundaries angles, (b) crystallographic orientations (IPF Z)



(a) (b)  
 Figure 5 : Evolution of the recrystallized  $\beta$ -Sn grains distribution with thermal cycling, (a) equivalent grain diameter range ( $\mu\text{m}$ ) and localization, (b) grains area proportion for different equivalent diameter ranges

This network of recrystallized grains spreads along the interface with the solder pad or along the diagonal until total recrystallization of the high strain area. This evolution leads to an attenuation of the initial macrograin texture induced by the progressive formation of more and more highly misoriented recrystallized grains during thermal cycling (Figure 4).

$\beta$ -Sn grains' size measurements have also been conducted using EBSD image analysis of joints with different damage levels. They show that new recrystallized tin grains size is between 1 and 30  $\mu\text{m}$  whatever the level of cycling (Figure 5.a). However, their population evolution in the highest stressed zone during thermomechanical cycling presents an increase in the recrystallized grains area percentage, which means the propagation of recrystallization throughout the joint. Figure 5.b shows that the recrystallized grains area for the first 1000 cycles does not exceed 5% of the whole solder area. Then, it is interesting to see that this percentage significantly rises until reaching 35% of the total joint surface at 1700 cycles.

### 3.2.3 Evolution of the $\text{Ag}_3\text{Sn}$ IMC particles

$\text{Ag}_3\text{Sn}$  IMCs coalescence is the other microstructural phenomenon that characterizes the thermomechanical damage. Under cycling,  $\text{Ag}_3\text{Sn}$  IMCs in the solder joints coarsen; the largest particles grow in size while smaller particles dissolve which leads to a loss of dendritic structure. This will decrease the precipitation hardening and make the solder softer, which facilitates the recrystallization [10].

$\text{Ag}_3\text{Sn}$  particles size and density were measured at different damage levels using EBSD analyses. Figure 6 shows an increase in  $\text{Ag}_3\text{Sn}$  IMCs equivalent diameter from  $\sim 0.3 \mu\text{m}$  to  $\sim 0.65 \mu\text{m}$  during thermal cycling which highlights the coarsening of the largest  $\text{Ag}_3\text{Sn}$  precipitates. In the other hand, the growth in the  $\text{Ag}_3\text{Sn}$  particles density observed until 1000 cycles may be explained by the coarsening of very small precipitates (diameter  $< 0.25 \mu\text{m}$ ) that were not detected in the very first cycles. Then this density drops because of the observed disappearance of the nano- $\text{Ag}_3\text{Sn}$  IMCs in the high stressed region from 1300 cycles. This is coupled with a growth of spacing between  $\text{Ag}_3\text{Sn}$  particles (Figure 9.b).

### 3.3. Crack evolution

Results show that crack initiation in BGA solder joints appear very early and could take place as soon as the recovery phase occurs. It was already observed in solder joints sampled between only 360 cycles and 1000 cycles in the geometrical singularity zones of the assembly near the joint neck.

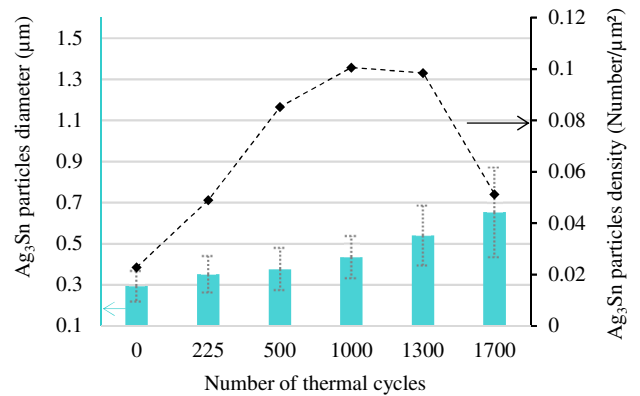


Figure 6 : Evolution of the  $\text{Ag}_3\text{Sn}$  particles population with thermal cycling

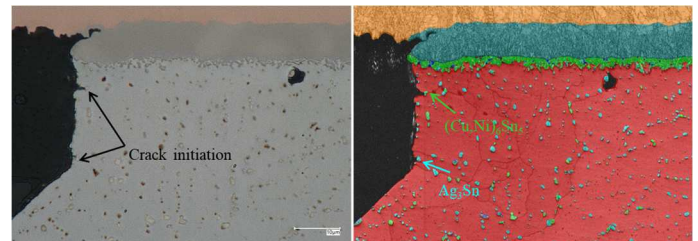


Figure 7 : Crack initiation site at 360 cycles

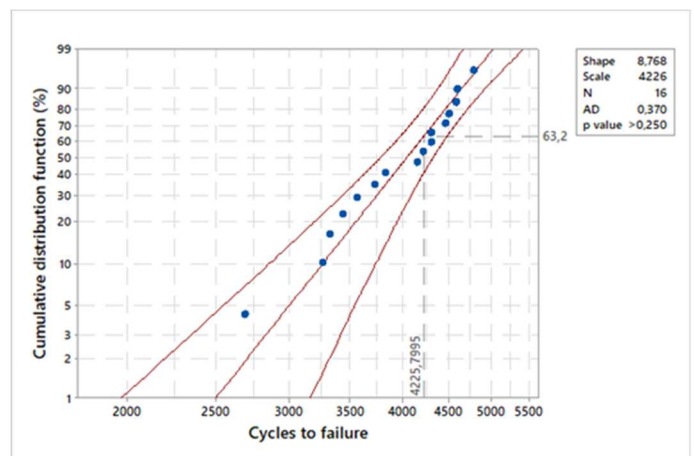


Figure 8 : Weibull distribution for the outermost joints row in BGA components

The presence of relatively large intermetallic particles in highly stressed areas also appears to facilitate crack initiation. EBSD mapping was made to characterize the crack initiation zone. The crystalline phases map shows the presence of large  $(\text{Cu,Ni})_6\text{Sn}_5$  and  $\text{Ag}_3\text{Sn}$  IMCs near the crack initiation site which can cause local brittleness in the solder (Figure 7 ). It is noteworthy that the crack initiation area was always characterized by the presence of IMCs in all analyzed samples. This was also observed on SAC solder joints of chip resistors assembled on



the same board and studied in similar test conditions [11].

The number of cycles after which crack initiation was observed in the various joints turns out to be very low compared to the measured lifetimes. The electrical monitoring of the outermost joints row of the same BGA components show that their measured fatigue lifetime is around 4225 cycles (Figure 8). This means that the crack initiation phase represents 9 to 24 % of the measured life and that solder fatigue lifetime is controlled by crack propagation.

After 1000 cycles, partial cracks were observed in the recrystallized area with low density of  $\text{Ag}_3\text{Sn}$  particles. Measurements revealed a significant increase of 18 % in the total recrystallized grains surface accompanied with a drop in  $\text{Ag}_3\text{Sn}$  precipitate density at 1300 cycles (Figure 5.a and Figure 6), that's was observed at the same time when first cracks (detected before 1000 cycles) start to propagate. This results show that a well-defined recrystallization amount coupled with an  $\text{Ag}_3\text{Sn}$  particle density threshold is required to trigger the intergranular cracks propagation (Figure 9).

As  $\text{Ag}_3\text{Sn}$  particles coarsening takes place, the dislocation motion is favored. After reflow, finely dispersed  $\text{Ag}_3\text{Sn}$  particles can proceed as barriers to the viscoplastic strain-induced dislocations motion and inhibit SAC305 solder degradation by dislocation pinning process [5][12]. However, with larger spacing between  $\text{Ag}_3\text{Sn}$  IMCs, the dislocations are no longer blocked, the largest particle can constitute good nucleation sites and recrystallization is accelerated. Moreover,  $\text{Ag}_3\text{Sn}$  precipitates tend to move towards high-disoriented grain boundaries as coalescence occurs. This migration weakens the grain boundaries leading to intergranular crack propagation.

#### 4. Conclusion

The investigations detailed in this study aim at giving a better comprehension of the as-reflowed microstructure and its evolution during thermomechanical loading. The global approach is based on an in-depth microstructural study of the evolving SAC305 BGA solder joint along thermomechanical fatigue using EBSD analyses at very early cycles (0 – 1700 cycles). A correlation with failure detection results of the same type of components allowed us to highlight the role played by each step of the failure mechanism from crack initiation until its propagation in the solder joints service life. According to observations performed along thermal cycling test, the failure mechanism in lead-free BGA solder joint can be summarized in three steps:

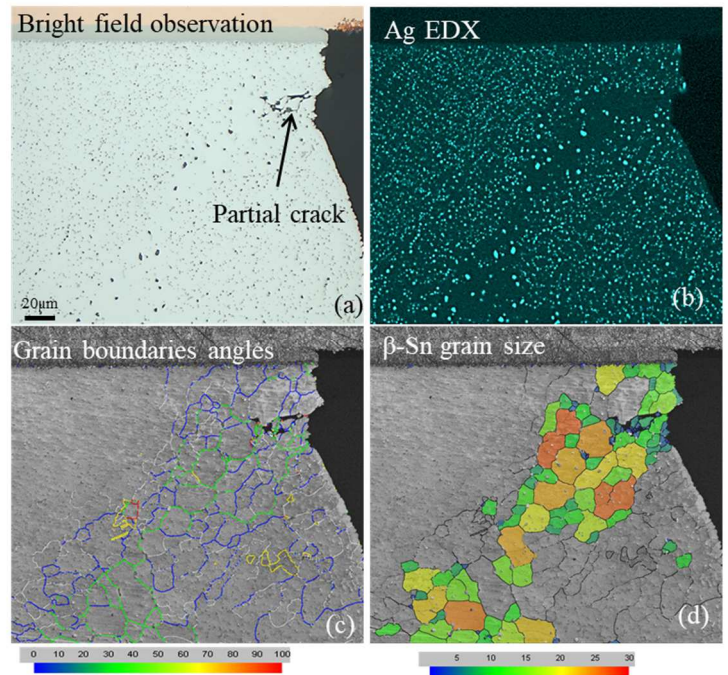


Figure 9 : Favorable intergranular crack path in BGA solder joint after 1300 cycles, (a, b)  $\text{Ag}_3\text{Sn}$  coarsening and migration, (c, d) network of highly misorientated recrystallized  $\beta\text{-Sn}$  grains

Firstly, a recovery process occurs in the high strain regions at the interface of the solder pads accompanied by a slight  $\text{Ag}_3\text{Sn}$  precipitates coarsening. Crack initiation also appear at the same time. This phase represents less than 24 % of BGA solder joint lifetime.

In the second step,  $\beta\text{-Sn}$  grains recrystallization with a high  $\text{Ag}_3\text{Sn}$  coarsening occur all the way through the highly stressed area until a well-defined recrystallization degree coupled with a threshold  $\text{Ag}_3\text{Sn}$  particle density value providing favorable intergranular propagation paths.

Finally, the intergranular cracks propagate in the network of highly misorientated recrystallized grains until complete cracking.

The study of other types of components (chip resistor and QFN) is also in progress in order to define a common microstructural damage criterion, which can be used in life prediction models.

#### Acknowledgements

This work is in the framework of the IRT Saint Exupery's research project FELINE. We acknowledge the financial and in-kind support (background knowledge and services) from the IRT Saint Exupery's industrial and academic members and the financial support of the French National Research Agency.

## References

- [1] T. Gu, C. M. Gourlay, and T. Ben Britton, "The Role of Lengthscale in the Creep of Sn-3Ag-0.5Cu Solder Microstructures," *J. Electron. Mater.*, vol. 50, no. 3, pp. 926–938, 2021.
- [2] T. T. Mattila and J. K. Kivilahti, "The role of recrystallization in the failure of SnAgCu solder interconnections under thermomechanical loading," *IEEE Trans. Components Packag. Technol.*, vol. 33, no. 3, pp. 629–635, 2010.
- [3] L. Yin, L. Wentlent, L. Yang, B. Arfaei, A. Qasaimeh, and P. Borgesen, "Recrystallization and precipitate coarsening in Pb-Free solder joints during thermomechanical fatigue," *J. Electron. Mater.*, vol. 41, no. 2, pp. 241–252, 2012.
- [4] J. B. Libot, J. Alexis, O. Dalverny, L. Arnaud, P. Milesi, and F. Dulondel, "Microstructural evolutions of Sn-3.0Ag-0.5Cu solder joints during thermal cycling," *Microelectron. Reliab.*, 2018.
- [5] P.-E. Tegehall, "Impact of solder pad finish and solder composition on the microstructure of solder joints to various types of components," no. December 2019, 2020.
- [6] E. Ben Romdhane, A. Guédon-Gracia, S. Pin, P. Roumanille, and H. Frémont, "Impact of crystalline orientation of lead-free solder joints on thermomechanical response and reliability of ball grid array components," *Microelectron. Reliab.*, vol. 114, no. October, p. 113812, 2020.
- [7] T. R. Bieler, H. Jiang, L. P. Lehman, T. Kirkpatrick, E. J. Cotts, and B. Nandagopal, "Influence of Sn Grain Size and Orientation on the Thermomechanical Response and Reliability of Pb-free Solder Joints," vol. 31, no. 2, pp. 370–381, 2008.
- [8] P. Roumanille, E. Ben Romdhane, S. Pin, P. Nguyen, J. Delétage, and A. Guédon-gracia, "Microelectronics Reliability Evaluation of thermomechanical fatigue lifetime of BGA lead-free solder joints and impact of isothermal aging," Accepted in *Microelectron. Reliab.*, 2021.
- [9] B. Zhou, T. R. Bieler, T. K. Lee, and K. C. Liu, "Crack development in a low-stress PBGA package due to continuous recrystallization leading to formation of orientations with [001] parallel to the interface," *J. Electron. Mater.*, vol. 39, no. 12, pp. 2669–2679, 2010.
- [10] T. K. Lee and H. Ma, "Aging impact on the accelerated thermal cycling performance of lead-free BGA solder joints in various stress conditions," *Proc. - Electron. Components Technol. Conf.*, pp. 477–482, 2012.
- [11] E. Ben Romdhane, P. Roumanille, A. Guédon-gracia, S. Pin, P. Nguyen, and H. Frémont, "Early microstructural indicators of crack initiation in lead-free solder joints under thermal cycling," 2021 IEEE 71nd Electronic Components and Technology Conference, pp. 2293–2301, 2021.
- [12] U. Sahaym, B. Talebanpour, S. Seekins, I. Dutta, P. Kumar, and P. Borgesen, "Recrystallization and Ag<sub>3</sub>Sn particle redistribution during thermomechanical treatment of bulk Sn-Ag-Cu solder alloys," *IEEE Trans. Components, Packag. Manuf. Technol.*, vol. 3, no. 11, pp. 1868–1875, 2013.